Research Article

Oliver Grothe and Na Luo*

Continuous displacement interpolation between checkerboard copulas

https://doi.org/10.1515/demo-2025-0018
Received June 10, 2025; accepted January 22, 2026; published online May 18, 2026

Abstract: This paper presents a displacement-like interpolation method between any two given checkerboard copulas. This interpolation is close to the geodesic connecting the two checkerboard copulas in the L^2-Wasserstein space, which, however, leaves the copula domain. In the proposed interpolation, mass is continuously shifted only across the boundaries of neighboring cells and copula property is ensured at each step. The method therefore can be interpreted as a discrete form of dynamical optimal transport constrained to the copula domain. We illustrate the interpolation with both a toy and a practical example, showing how the method yields dependence structures between two known states.

Keywords: displacement interpolation; checkerboard copula; dynamical optimal transport

MSC 2020: MSC 2020 Primary; 62H05 Secondary; 62H20; 49Q22

1 Introduction

Copulas are fundamental statistical tools used to model the dependence between random variables, with a wide range of applications in finance (Cherubini et al. 2004; Genest et al. 2009; Patton 2012), hydrology (Cong and Brady 2012; Tootoonchi et al. 2020), climate and weather research (Schoelzel and Friederichs 2008), astronomy (Yuan et al. 2018), and so on. In general dependence modeling studies, the data used to build models are typically available only under a limited number of conditions. As a result, copula models can only be built for these distinct states. For example, Coblenz et al. (2020) develops 10 fuel injector spray copula models for different operating conditions of an aircraft turbine, while Patton (2012) constructs copula models at a series of time points. Given these distinct copula models, researchers would like to obtain a unified dependence structure that extends to all states, including those without available data. A feasible approach is to interpolate among the existing copula models. In particular, for two distinct states, a suitable interpolation between their corresponding copula models is crucial for understanding how the dependence structure evolves.

A simple and feasible choice that immediately comes to mind maybe the linear interpolation, as the linear interpolant of any two copulas with weights $(t, 1-t)$ remains within the copula domain. However, this approach is just a simple mix of the two copulas, and often can not reflect the evolution process effectively. A second approach is parameter-based interpolation, as suggested in Coblenz et al. (2020) for fuel injector spray modeling. In this method, an overarching dependence structure is required, meaning that the copulas must belong

***Corresponding author: Na Luo**, Institute of Operations Research, Analytics and Statistics, Karlsruhe Institute of Technology, Kaiserstr. 12, 76131, Karlsruhe, Germany, E-mail: na.luo@kit.edu
Oliver Grothe, Institute of Operations Research, Analytics and Statistics, Karlsruhe Institute of Technology, Kaiserstr. 12, 76131 Karlsruhe, Germany

to a same parametric family to allow interpolation of their parameters. This constraint makes it unsuitable for interpolating between different classes of copulas. The kind of interpolation we look for in this paper is displacement interpolation, which is related to an optimal transport path describing the transport of a unit "mass" from one distribution to another along a vector field while satisfying local mass conservation laws. It therefore provides a physically meaningful way to model the evolution process. For this method, a key challenge is that the displacement interpolation of two copulas almost always falls outside the copula domain.

The aim of this work is therefore to seek an interpolation that is a valid copula and lies "in between" any two given copulas, effectively capturing the continuous evolution process, particularly through the optimal transport path and its related variants. Recently, several studies have investigated the interplay between copulas and optimal transport – for instance, employing copulas to approximate optimal transport maps for continuous densities (Chi et al. 2019, 2022), analyzing the optimal transport between probability measures sharing the same copula and its extensions to orthogonal transformations (Alfonsi and Jourdain 2014; Ghaffari and Walker 2021), and defining intra-Earth Mover's distances between copulas for clustering purposes (Marti et al. 2016). To the best of our knowledge, however, there has been no prior work that explicitly formulates and utilizes optimal transport path within the copula domain to construct interpolation between copulas, which we think makes our research novel and meaningful.

We address the interpolation problem specifically for checkerboard copulas, a special class of copula whose density is uniformly distributed on multiple uniform subdivisions of the unit square (Kuzmenko et al. 2020), where certain mathematical tools can be applied. Our results are general, as the set of checkerboard copulas is dense in the copula domain (Durante et al., 2016; Li et al. 1997). Moreover, in recent years, significant research has focused on the development and application of checkerboard copulas, such as the paper Kuzmenko et al. (2020) explores the use of checkerboard copulas to model multivariate distributions, the paper Grothe and Rieger (2024) focuses on analyzing their dependence structures, and the paper Perrone et al. (2019) shows how to select (checkerboard) copulas that have the maximum entropy and are ultramodular using the polytopal representation of ultramodular discrete copulas.

In constructing our displacement-like interpolation, the key point is that the probability mass should move continuously, resembling the flow of physical particles or a liquid along a vector field which satisfies the continuity equation. We achieve this by employing dynamical optimal transport, and utilizing the inverse statement of the well-known Sklar's theorem (Sklar 1959), which is computationally efficient for checkerboard copulas, to ensure that the evolving distribution remains within the copula domain. Additionally, we introduce a new concept called "adjacent mass-movement," which restricts the probability mass to move only across adjacent cells of the checkerboard, ensuring that mass does not jump or disappear during the interpolation process. As a result, the interpolation we obtained closely follows the optimal transport path in terms of the L^2-Wasserstein distance, preserving both the continuity of mass movement and the underlying dependence structure. Moreover, due to the continuity constraint in the mass movement, certain copula functionals also exhibit corresponding continuous behavior. For example, the corresponding Kendall's τ and Spearman's ρ generally show a gradual and relatively smooth increase or decrease throughout the interpolation, depending on the initial and final copulas.

In this paper, we first show that continuous, i.e., mass transport is restricted to neighboring cells, interpolation between any two checkerboard copulas is theoretically possible while staying in the copula domain. This motivates a heuristic approach to construct an explicit continuous path which has continuity with respect to the max-norm. However, finding an optimal, i.e., shortest, continuous interpolation that remains entirely within the copula domain is generally infeasible. To address this, we guide the interpolation along the direct Wasserstein geodesic, which lies outside the copula space, by selecting a discrete sequence of points along the geodesic and transforming them into checkerboard copulas. These copulas are then connected via local interpolations between adjacent ones, yielding a continuous path that remains within the copula domain and closely follows the geodesic.

For clarity of presentation, we develop most of our results in the two-dimensional setting, where constructions can be visualized and explained more transparently. Nevertheless, the underlying ideas extend naturally to higher dimensions, as discussed in Section 3.3.

The rest of the paper is organized as follows. Section 2 introduces the fundamentals of copulas and the optimal transport problem. In Section 3, we prove that any two 2-dimensional checkerboard copulas can be connected through a sequence of adjacent mass movements, and we provide a detailed construction of this process for both the two- and higher-dimensional cases. Section 4 explores the interpolation induced by optimal transport. Section 5 presents two examples to illustrate the final displacement-like interpolation. Finally, we conclude the study and propose potential directions for future research.

2 Preliminaries

Since our detailed analysis focuses on the two-dimensional case, we present the concepts and notation in 2D whenever this does not cause any conceptual loss. The multivariate generalization follows the same principles and is discussed later in Section 3.3.

2.1 Copula and Sklar's theorem

A copula is a joint cumulative distribution function (CDF) with standard uniform univariate margins. From an analytical perspective, a copula is a function $C : [0,1]^2 \to [0,1]$ with following properties:

1. For $\forall u, v \in [0,1]$,
$$C(u,0) = C(0,v) = 0, \quad C(u,1) = u, \quad \text{and} \quad C(1,v) = v. \tag{1}$$
2. C is 2-increasing, i.e., for $\forall u_1, u_2, v_1, v_2 \in [0,1]$ such that $u_1 \le u_2$ and $v_1 \le v_2$,
$$C(u_2,v_2) - C(u_2,v_1) - C(u_1,v_2) + C(u_1,v_1) \ge 0. \tag{2}$$

Let H be the CDF of real random variables X and Y with respective margins F, G. According to the well-known Sklar's theorem (Sklar 1959), there exists a copula C such that for $x, y \in \overline{\mathbb{R}}$,

$$H(x,y) = C(F(x), G(y)). \tag{3}$$

Especially, C is unique when F and G are continuous. The copula corresponding to a joint distribution function H with continuous margins F and G can be expressed as

$$C(u,v) = H\big(F^{(-1)}(u), G^{(-1)}(v)\big) \quad \text{for} \quad (u,v) \in [0,1]^2, \tag{4}$$

where $F^{(-1)}$ and $G^{(-1)}$ are the quasi-inverses of F and G defined by

$$F^{(-1)}(t) = \inf\{x | F(x) \ge t\}, \quad G^{(-1)}(t) = \inf\{x | G(x) \ge t\} \quad \text{for} \quad t \in [0,1]. \tag{5}$$

From Sklar's theorem, we know that any joint distribution can be decomposed into its univariate margins and a corresponding copula, which reflects the dependence between the random variables.

As a copula captures the dependence structure between random variables, a pure measure of dependence should depend only on the copula and not on the marginal distributions. For further discussion of dependence measures, we refer the reader to Scarsini (1984), Schmid et al. (2010), and Grothe et al. (2014). Two widely used copula-based dependence measures that satisfy this criterion are Spearman's ρ_s and Kendall's τ, which can be computed as

$$\rho_s = 12 \int_0^1 \int_0^1 C(u,v) - uv \mathrm{d}u\mathrm{d}v, \quad \text{and} \quad \tau = 4 \int_0^1 \int_0^1 C(u,v) \mathrm{d}C(u,v) - 1. \tag{6}$$

For a more general introduction to copulas and copula-based modeling – including their construction, properties, and applications – we refer the reader to Nelsen (2006) and Joe (2014).

2.2 Checkerboard copula

A checkerboard copula is a special type of copula whose density remains constant within each cell of a uniform subdivision of the unit square (Kuzmenko et al. 2020). For simplicity, consider a subdivision with size $I_N \times I_N$, where $I_N = \{0, 1/N, 2/N, \dots, 1\}$. Then the set of checkerboard copulas has a one-to-one correspondence relationship with the set of doubly stochastic matrices $\mathcal{S}_N \subset \mathbb{R}^{N\times N}$. First, any copula C defines a doubly stochastic matrix A by

$$A_{ij} = N\left[C\left(\frac{i}{N}, \frac{j}{N}\right) - C\left(\frac{i-1}{N}, \frac{j}{N}\right) - C\left(\frac{i}{N}, \frac{j-1}{N}\right) + C\left(\frac{i-1}{N}, \frac{j-1}{N}\right)\right] \quad \text{for } i, j = 1, 2, \dots, N. \tag{7}$$

It is straightforward to verify that $A \in \mathcal{S}_N$: The non-negativity of each entry in A follows from the 2-increasing property given in Equation (2), while the conditions $\sum_{i=1}^{N} A_{ij} = 1$ and $\sum_{j=1}^{N} A_{ij} = 1$ are ensured by Equation (1). Conversely, any doubly stochastic matrix $A \in \mathcal{S}_N$ defines a checkerboard copula C^{ck} via

$$C^{ck}(u, v) = \int_0^u \int_0^v c(s, t)\mathrm{d}t\mathrm{d}s \quad \text{for} \quad (u, v) \in [0, 1]^2 \tag{8}$$

where the density $c(u, v)$ is a step function that remains constant within each cell $\left(\frac{i-1}{N}, \frac{i}{N}\right] \times \left(\frac{j-1}{N}, \frac{j}{N}\right]$, and is given by

$$c(u, v) = NA_{ij} \quad \text{for} \quad (u, v) \in \left(\frac{i-1}{N}, \frac{i}{N}\right] \times \left(\frac{j-1}{N}, \frac{j}{N}\right]. \tag{9}$$

It is easy to verify that C^{ck} satisfies properties (1) and (2), and therefore qualifies as a copula, specifically a checkerboard copula.

Therefore, any checkerboard copula can be represented by a doubly stochastic matrix $A \in \mathcal{S}_N$, where each entry A_{ij} denotes the probability mass of the corresponding cell in the subdivision. In the following, unless otherwise mentioned, we denote a checkerboard copula simply as $A \in \mathcal{S}_N$. Moreover, for any fixed copula, formula (7) provides a discretization method to obtain its corresponding checkerboard copula $A_N \in \mathcal{S}_N$. As $N \to \infty$, this sequence of checkerboard copulas A_N approximates the original copula (Li et al. 1997).

The matrix representation also facilitates the computation of dependence measures. In particular, Durrleman et al. (2000) shows that the Spearman's ρ_s and Kendall's τ of a checkerboard copula $A \in \mathcal{S}_N$ can be computed by

$$\begin{aligned} \tau(A) &= 1 - \frac{1}{N^2}\mathrm{trace}\left(BABA^T\right) \\ \rho(A) &= \frac{3}{N}\mathrm{trace}(\Theta A) - 3 \end{aligned} \tag{10}$$

where A^T is the transpose of A, and $B \in \mathbb{R}^{N\times N}$ is defined as

$$B_{ij} = \begin{cases} 1 & \text{if } i = j \\ 2 & \text{if } i > j \\ 0 & \text{if } i < j, \end{cases}$$

and $\Theta \in \mathbb{R}^{N\times N}$ is given by

$$\Theta_{ij} = \frac{1}{N^2}(2N - 2i + 1)(2N - 2j + 1).$$

2.3 Optimal transport and displacement interpolation

Optimal transport is a well-developed mathematical theory that defines a family of metrics between probability distributions, with successful theoretical analysis and a wide range of computational applications (Peyré et al.,

2019; Santambrogio 2015; Villani et al. 2008). For two given probability measures $\mu_0, \mu_1 \in \mathcal{P}(\Omega)$, and a cost function $d: \Omega \times \Omega \to [0, +\infty]$, the optimal transport problem is

$$\inf_{\pi \in \Pi(\mu_0, \mu_1)} \int_{\Omega \times \Omega} d(x, y) \mathrm{d}\pi(x, y) \tag{11}$$

where $\pi \in \Pi(\mu_0, \mu_1)$ is a measure on $\Omega \times \Omega$ with margins μ_0 and μ_1, called a transport plan. When the cost function is $d(x, y) = \|x - y\|^p$, the optimal value of (11) corresponds to the p-th power of the Wasserstein p-distance between μ_0 and μ_1, denoted as $W_p^p(\mu_0, \mu_1)$.

For the general continuous setting, we assume that the two given probability measures μ_0 and μ_1 both have density f_0 and f_1 on Ω respectively, where $\Omega \subset \mathbb{R}^2$ is a convex and compact domain. Note that the checkerboard copula satisfies this condition, as its density is almost continuously defined on the unit square domain. According to the Benamou-Brenier formula (Benamou and Brenier 2000), the 2-nd power of the Wasserstein distance $W_2^2(\mu_0, \mu_1)$ is equal to twice the minimum value of:

$$\begin{aligned} \min_{f, \mathbf{v}} \quad & \frac{1}{2} \int_0^1 \int_\Omega f(t, x) \|v(t, x)\|^2 \mathrm{d}x \mathrm{d}t, \\ \text{subject to} \quad & \partial_t f + \nabla_x \cdot (f v) = 0, \\ & f(0, \cdot) = f_0, \quad f(1, \cdot) = f_1, \end{aligned} \tag{12}$$

where both f and v are defined on the time–space domain $[0, 1] \times \Omega$. The first constraint represents the continuity equation, while the second specifies the prescribed initial and terminal conditions. This problem is referred to as the dynamical optimal transport problem. In this framework, $f(t, \cdot)$ represents an interpolation path connecting the initial density $f(0, \cdot)$ and the final density $f(1, \cdot)$. The function $v(t, \cdot) = \left(v^1(t, \cdot), v^2(t, \cdot)\right)$ is a two-dimensional vector field that describes the flow of the density $f(t, \cdot)$. The term $\nabla_x \cdot v = \partial_{x_1} v^1 + \partial_{x_2} v^2$ denotes the divergence, where $x = \left(x_1, x_2\right)$ is the spatial coordinates. For example, $f(0.5, \cdot)$ describes the density at the midpoint of the interpolation, while $v(0.5, \cdot)$ represents the corresponding vector field that governs the flow at that instant. Similarly, as $\epsilon \to 0$, $v(0.5 + \epsilon, \cdot)$ characterizes the next infinitesimal step in the evolution of the flow.

Note that the optimal transport plan π in problem (11) can be constructed from the flows $(f(t, \cdot), v(t, \cdot))$, the solution of the problem (12). Specifically, consider the map $Y_t: \Omega \to \Omega$ induced by $v(t, \cdot)$ as the solution of the ordinary differential equation

$$\begin{cases} \dfrac{\mathrm{d}Y_t(x)}{\mathrm{d}t} = v(t, Y_t(x)) \\ Y_0(x) = x. \end{cases} \tag{13}$$

Then the measure $\mu_t = (Y_t)_{\#}\mu_0$ connects μ_0 and μ_1, and its corresponding density is f_t, where $(Y_t)_{\#}$ denotes the push-forward of μ_0 by the measurable map Y_t. Taking $t = 1$, the optimal transport plan is $\pi = (id, Y_1)_{\#}\mu_0$. Conversely, the pair $(f(t, \cdot), v(t, \cdot))$ can also be constructed from π, and we refer to Santambrogio (2015, cha. 5) for more details.

The solution $f(t, \cdot)$ of the dynamical optimal transport problem (12) is the geodesic between f_0 and f_1 in the Wasserstein space $\mathcal{W}_2(\Omega)$. It is also known as displacement interpolation. The dynamical optimal transport problem remains challenging due to its high computational cost. There are several algorithms relying on discretizations to solve it, such as the alternating direction method multiplier method (ADMM) proposed by Benamou and Brenier (2000), the Douglas-Rachford algorithm, and primal-dual splitting schemes studied in paper (Papadakis et al. 2014).

Less challenging is the situation where both, μ_0 and μ_1, are discrete measures, and defined as

$$\mu_0 = \sum_{i=1}^n a_i \delta_{x_i} \text{ and } \mu_1 = \sum_{j=1}^m b_j \delta_{y_j}. \tag{14}$$

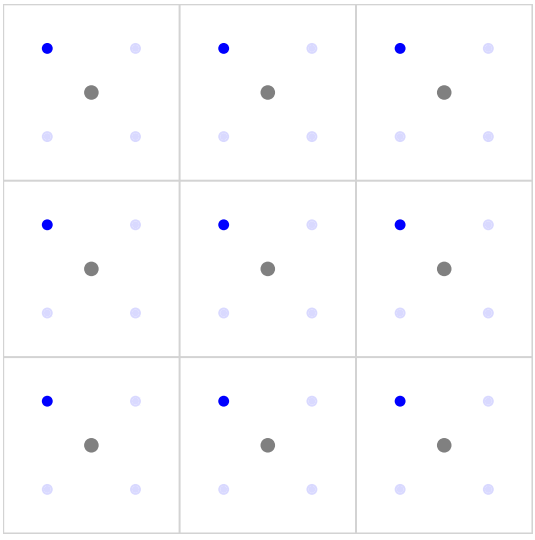

Figure 1: The discretization of a checkerboard copula with size $N = 3$. The gray dots are the discretization with size I_3, and the blue dots are the finer discritization with size I_6.

Here δ_{x_i} and δ_{y_j} denote Dirac measures centered at points x_i and y_j respectively. The Wasserstein p-distance between μ_0 and μ_1 is given by:

$$W_p^p(\mu_0, \mu_1) = \min_P \sum_{i,j} P_{ij} \left\| x_i - y_j \right\|^p, \tag{15}$$

where P is a transport plan, satisfying the marginal constraints: $\sum_j P_{ij} = a_i$, $\sum_i P_{ij} = b_j$, and $P_{ij} \geq 0$. For this discrete optimal transport problem, several solution methods are available, including the network simplex algorithm, the dual ascent method, and the auction algorithm (Peyré et al. 2019).

Note that we can relate a checkerboard copula A naturally to a discrete measure as above because its density is piecewise constant within each cell of the grid. Specifically, we can concentrate the total mass in any cell $\left(\frac{i-1}{N}, \frac{i}{N}\right] \times \left(\frac{j-1}{N}, \frac{j}{N}\right]$ at its center $x_{ij} = \left(\frac{2i-1}{2N}, \frac{2j-1}{2N}\right)$, as illustrated by the gray dots in Figure 1. Then the corresponding discrete measure is given by

$$\mu_A = \sum_{i,j=1}^{N} A_{ij} \delta_{x_{ij}} = \sum_{k=1}^{N^2} A_k \delta_{x_k}, \text{ where } k = (i-1)N + j. \tag{16}$$

Therefore, for two checkerboard copulas $A_0, A_1 \in \mathcal{S}_N$, the p-Wasserstein distance between their corresponding discrete measures as defined above is well-defined, with the cost function

$$d(x_k, x_{k'}) = \left\| x_k - x_{k'} \right\|^p = \left\| x_{ij} - x_{i'j'} \right\|^p. \tag{17}$$

Furthermore, we can construct a finer discretization of a checkerboard copula. For example, we can discretize it with a grid of size $I_{2N} \times I_{2N}$, which means that each cell of the original $N \times N$ subdivision is divided into four smaller cells. The mass in each smaller cell is then $\frac{1}{4}$ of the mass in the corresponding original cell. This finer discretization is represented by the blue dots in Figure 1, and we denote the corresponding discrete measure as $\mu_{A,2N}$. For the Wasserstein distances between the discrete measures from these two levels of discretization, we have the inequality

$$W_p\left(\frac{\mu_{A_0,2N}}{2N}, \frac{\mu_{A_1,2N}}{2N}\right) \leq W_p\left(\frac{\mu_{A_0}}{N}, \frac{\mu_{A_1}}{N}\right), \quad 1 \leq p < \infty. \tag{18}$$

Note that the value A_{ij}/N is the true probability mass of the copula $A \in \mathcal{S}_N$ in the (i, j)-cell. This inequality can be justified as follows: the relative positions and distances among the centers of the upper left subcells in each original cell (represented by the brighter blue dots in Figure 1) are the same as those among the centers of the original cells (the gray dots). Furthermore, the mass at each of these brighter blue dots is one-fourth of the mass at the corresponding gray dot. Therefore, the optimal transport plan for the gray dots also induces a feasible

transport plan for the brighter blue dots, with the total cost being exactly $\frac{1}{4}$ of the original. Since each original cell is split into four subcells (upper left, upper right, lower left, and lower right), the original optimal transport plan can be extended to a valid plan between the new centers. Thus, we obtain a transport plan whose cost is equal to $W_p(\frac{\mu_{A_0}}{N}, \frac{\mu_{A_1}}{N})$. Since other (potentially more optimal) plans may exist on the finer scale, inequality (18) follows. As the Wasserstein distance between general measures can be approximated through finer and finer discretizations, we obtain the inequality

$$W_p\Big(\frac{\mu_{A_0}}{N}, \frac{\mu_{A_1}}{N}\Big) \geq W_p\Big(\frac{\mu_{A_0,2N}}{2N}, \frac{\mu_{A_1,2N}}{2N}\Big) \geq \ldots \geq W_p\Big(\frac{\mu_{A_0,2^mN}}{2^mN}, \frac{\mu_{A_1,2^mN}}{2^mN}\Big) \geq \ldots, \tag{19}$$

and convergence

$$W_p\Big(\frac{\mu_{A_0,2^mN}}{2^mN}, \frac{\mu_{A_1,2^mN}}{2^mN}\Big) \to W_P(f_0, f_1) \quad \text{as } m \to \infty, \tag{20}$$

where f_0, f_1 are the densities corresponding to the checkerboard copulas A_0, A_1.

3 Continuous interpolation between checkerboard copulas

In this section, we prove that any two checkerboard copulas can be connected by a sequence of adjacent mass movements, which is called continuous interpolation. Furthermore, we give a detailed construction of a continuous interpolation path.

3.1 Existence of continuous interpolation based on adjacent mass-movement

In order to prove the existence of continuous interpolation, we first introduce the basic adjacent mass movements concept. In the Markov basis within the framework of $N \times N$ independence model for two-way contingency tables, a ***basic mass movement*** is defined as a integer matrix $Z = Z(i_1, i_2;\ j_1, j_2) = Z_{ij}$ as follows (Aoki et al. 2012, Cha2.),

$$Z_{ij} = \begin{cases} +1 & (i,j) = (i_1, j_1), (i_2, j_2), \\ -1 & (i,j) = (i_1, j_2), (i_2, j_1), \\ 0 & \text{otherwise.} \end{cases} \tag{21}$$

For a positive real number $a > 0$ and a checkerboard copula A, we consider the new matrix

$$\tilde{A} := A + aZ(i_1, i_2; j_1, j_2). \tag{22}$$

This process can be regarded as the mass "a" in the (i_1, j_2)- and (i_2, j_1)-cells being transported to the (i_1, j_1)- and (i_2, j_2)-cells, respectively. Note that every row and column of $\tilde{A}$ sums to 1; and thus if all the elements of $\tilde{A}$ are non-negative, we get a new checkerboard copula $\tilde{A}$. For this case, we say that $aZ(i_1, i_2;\ j_1, j_2)$ ***can be added to*** the checkerboard copula A (Aoki et al. 2012, cha. 4). We now define the basic adjacent mass movement and the continuous interpolation between checkerboard copulas.

Definition 3.1. $Z(i_1, i_2;\ j_1, j_2)$ is called a **basic adjacent mass movement**, if it belongs to

$$\mathcal{B} := \big\{Z(i_1, i_2; j_1, j_2) : |i_1 - i_2| = 1 \text{ or } |j_1 - j_2| = 1\big\}. \tag{23}$$

If $Z \in \mathcal{B}$ is a basic adjacent mass movement and βZ can be added to a checkerboard copula A, then the new checkerboard copula $\tilde{A} = A + \beta Z$ is obtained by transporting a mass "β" between two neighboring cells of A; this is why we refer to Z as an adjacent mass movement. Moreover, since $\beta \in \mathbb{R}$, we may transport any intermediate amount $\beta_s \leq \beta$; for example $\beta_s = s\beta$ for $s \in [0, 1]$, which illustrates the notion of "continuity". This interpolation

also captures the idea of a physical mass displacement: mass is conserved at every intermediate stage and moves continuously, without disappearance or abrupt jumps.

Definition 3.2. A **continuous interpolation** between two checkerboard copulas A_0 and A_1 is a connecting path consisting of a sequence of basic adjacent mass movements $Z_1, \dots, Z_I \in \mathcal{B}$, satisfying

$$A_1 = A_0 + \sum_{i=1}^{I} \beta_i Z_i, \tag{24}$$

where $\beta_i > 0$, and $\beta_i Z_i$ can be added to $A_0 + \sum_{j=1}^{i-1} \beta_j Z_j$ for $i = 1, \dots, I$. We define the quantity $\frac{2\sum_{i=1}^{I}\beta_i}{N}$ as the **transport effort** associated with this interpolation.

The transport effort refers to the cost of the transport plan induced by the interpolation, where the cost function is the L^1 norm $d(x, y) = \|x - y\|$. If we regard checkerboard copulas as discrete measures, then any feasible continuous interpolation (24) induces a transport plan from μ_{A_0} to μ_{A_1}. At each step of such an interpolation, a total $2\beta_i$ mass is transported due to the bidirectional nature of movement between adjacent cells. As the transport cost is given by the L^1-norm, each such transport step incurs a cost of $\frac{1}{N}$. Consequently, the total transport cost is $\frac{2\sum_{i=1}^{I}\beta_i}{N}$. Furthermore, since the Wasserstein-1 distance is the minimal total cost among all possible transport plans, we obtain the following inequality between the Wasserstein-1 distance and the transport effort associated with any feasible continuous interpolation:

$$\text{transport effort} \geq W_1(\mu_{A_0}, \mu_{A_1}). \tag{25}$$

This inequality reflects the price we need to pay to remain within the copula domain.

The formula (24) effectively shows that the mass can be transported from A_0 to A_1 in a continuous manner without abrupt jumps, even though the path is expressed as a finite sum of basic adjacent mass movements. This is because, at each step, the transported mass β_i is a real-valued quantity, and it can be continuously adjusted to any value up to β_i when moving between adjacent cells. Hence the total transport can be realized via a sequence of infinitesimal adjustments that never create or annihilate mass.

In what follows, we formalize this observation and provide a constructive proof of the existence of a continuous interpolation.

Proposition 3.3. *There exist a continuous interpolation between any two checkerboard copulas A_0 and A_1, where "continuous" means that the transported mass evolves without jumps or disappearance, i.e., at every intermediate time the mass moves through adjacent cells in a continuous fashion as described above.*

Proof. According to Birkhoff's theorem, every doubly stochastic matrix can be represented as a convex combination of permutation matrices (Birkhoff 1946). Therefore, any checkerboard copula A can be expressed as

$$A = \sum_{k=1}^{K} \alpha_k P_k \quad \alpha_k > 0, \tag{26}$$

where $K \leq N^2$, $\sum_{k=1}^{K} \alpha_k = 1$, and all P_k are N-th order permutation matrices (Kolesárová et al. 2006). Note that the identity matrix can be obtained from any permutation matrix P_k, by successively exchanging adjacent columns in at most $(N-1)!$ steps. And every exchange is equal to add an adjacent mass movement $Z \in \mathcal{B}$ to P_k: if j-th and $(j+1)$-th columns are exchanged and $(P_k)_{i_1 j} = (P_k)_{i_2 j+1} = 1$, then this process is equal to add $Z := Z(i_2, i_1; j, j+1) \in \mathcal{B}$ to P_k. Therefore, there exists a finite sequence of adjacent mass movements Z_i, such that $P_k + \sum_{i=1}^{I_k} Z_i = E$, where E is the identity matrix. And furthermore we have

$$A + \sum_{k=1}^{K} \alpha_k \left(\sum_{i=1}^{I_k} Z_i \right) = \sum_{k=1}^{K} \alpha_k \left(P_k + \sum_{i=1}^{I_k} Z_i \right) = E. \tag{27}$$

As each step in this process is an exchange of adjacent columns of a permutation matrix P_k, the non-negativity of the new matrix is preserved. This ensures the existence of an interpolation between any given checkerboard copula A and E. For A_0 and A_1, we first construct an interpolation between A_0 and E, and then between E and A_1. Thus, we finish the proof of the Proposition 3.3. □

Remark 1. In this proof, we use the fact that any permutation matrix P can be transformed into the identity matrix by a finite sequence of adjacent column exchanges, where each exchange corresponds to an adjacent mass movement. To clarify this, we now provide an example:

$$P \equiv \begin{bmatrix} 0 & 0 & 1 & 0 \\ 1 & 0 & 0 & 0 \\ 0 & 1 & 0 & 0 \\ 0 & 0 & 0 & 1 \end{bmatrix} \to \begin{bmatrix} 0 & 1 & 0 & 0 \\ 1 & 0 & 0 & 0 \\ 0 & 0 & 1 & 0 \\ 0 & 0 & 0 & 1 \end{bmatrix} \to \begin{bmatrix} 1 & 0 & 0 & 0 \\ 0 & 1 & 0 & 0 \\ 0 & 0 & 1 & 0 \\ 0 & 0 & 0 & 1 \end{bmatrix},$$

The first step exchanges the 2nd and 3rd columns, and the second step exchanges the 1st and 2nd columns. These two exchanges correspond to two sequential adjacent mass movements:

$$P + Z(1,3;2,3) + Z(1,2;1,2) = P + \begin{bmatrix} 0 & 1 & -1 & 0 \\ 0 & 0 & 0 & 0 \\ 0 & -1 & 1 & 0 \\ 0 & 0 & 0 & 0 \end{bmatrix} + \begin{bmatrix} 1 & -1 & 0 & 0 \\ -1 & 1 & 0 & 0 \\ 0 & 0 & 0 & 0 \\ 0 & 0 & 0 & 0 \end{bmatrix} = E.$$

Remark 2. This proof gives a method for constructing a continuous interpolation between A_0 and A_1. The process involves expressing both matrices as combinations of permutation matrices and then sequentially connecting them to the identity matrix through column exchanges. However, it is not a direct construction, as it introduces a third checkerboard copula E. Furthermore, the transport effort $2\sum_{i=1}^{I}\beta_i/N$ in this construction is the sum of the transport effort between A_0 and E and that between E and A_1. As a result, the transport effort of this interpolation has no continuity with respect to the max-norm, i.e., the transport effort does not necessarily tend to zero when $\|A_n - A\|_{\max} := \max |A_n - A|_{ij} \to 0$. This discontinuity suggests that small perturbations in A may still lead to non-negligible transport effort, making the interpolation method less desirable.

3.2 Construction of a concrete continuous interpolation path

To overcome the limitations of the interpolation discussed in Remark 2, we now introduce a direct construction of a continuous interpolation that does not route through the identity matrix. This construction will ensure the continuity of the transport effort with respect to the max-norm. From this point of view, this is a more natural and efficient interpolation. We now provide the detailed construction, starting with a preliminary connection involving basic but non-adjacent movements, which are then refined into adjacent movements in a second stage.

3.2.1 Decompose to a sequence of basic mass movements

Assume that A_0 and A_1 are the two checkerboard copulas to be interpolated. We connect them by a sequence of mass movements:

$$A_1 = A_0 + \sum_{r=1}^{R} a_r Z(i_r, k_r; l_r, j_r), \tag{28}$$

where $R \le N^4$, $0 < a_r \le 2^R \|A_1 - A_0\|_{\max}$, and $A_0 + \sum_{r=1}^{R_0} a_r Z(i_r, k_r; l_r, j_r)$ remains within the checkerboard copula domain at each steps $R_0 \le R$. Here, $Z(i_r, k_r;\ l_r, j_r)$ represents a basic mass movement, which is not necessarily adjacent. This can be achieved through the following process:

1. let $D = A_1 - A_0$ represent the difference between the two checkerboard copulas. Since both A_0 and A_1 are doubly stochastic matrices, every row and column of D sums to zero. If all elements in the first row of D are zero, move to the next row. Otherwise, the first row must contain both negative and positive elements. Identify the smallest (most negative) and largest (most positive) elements in the first row, denoted as $D_{1j} < 0$ and $D_{1l} > 0$, respectively. Then, find the smallest (most negative) element in the l-th column, denoted as $D_{kl} < 0$. This process is visually represented as follows:

$$\begin{array}{c} \\ 1 \\ k \end{array} \begin{array}{c} \begin{array}{cc} j & l \end{array} \\ \begin{bmatrix} - & + \\ . & - \end{bmatrix} \end{array}.$$

This corresponds to a natural mass movement $Z(1, k;\ l, j)$. Now, define

$$a_1 = \min\{-D_{1j}, D_{1l}, -D_{kl}\}. \tag{29}$$

By construction, it is straightforward to verify that $A_0 + a_1 Z(1, k;\ l, j)$ remains a valid checkerboard copula. At this stage, we have

$$A_1 = A_0 + a_1 Z(1, k; l, j) + \tilde{D}, \tag{30}$$

where $\tilde{D} \equiv D - a_1 Z(1, k; l, j)$. By the definition of a_1, we know that $a_1 \le \|D\|_{\max}$, which further implies that $\left\|\tilde{D}\right\|_{\max} \le 2\|D\|_{\max}$. This shows that after performing one mass movement step, the maximum absolute value in the updated difference matrix does not increase by more than a factor of 2.

2. If there are still nonzero elements in the first row of $\tilde{D}$, we repeat the above procedure. For the second mass movement step, we have $a_2 \le 2\left\|\tilde{D}\right\|_{\max} \le 2^2\|D\|_{\max}$. This iterative process continues until all elements in the first row of the difference matrix are zero. The procedure terminates within at most $(N-1)^3$. This bound is established as: The first row of the original difference matrix D contains at most $N-1$ negative elements; For each negative element in the first row, there are at most $N-1$ corresponding positive elements in the same row; Each of these positive elements, in turn, has at most negative elements in its respective column.
3. We now proceed to the second row and apply the same operation. The number of steps required for the second row is at most $(N-1)(N-2)^2 \le (N-1)^3$. Since the first row is already zero, this process does not affect it.
4. We then continue sequentially with the remaining rows until all elements in the difference matrix are zero. Thus, the total number of mass movement steps is bounded by $R \le (N-1)^4 \le N^4$, and each step satisfies $a_r \le 2^R\|D\|_{\max}$ for $r \le R$.

Example 1. We provide an example to illustrate the above process. Consider the checkerboard copulas:

$$A_0 = \begin{bmatrix} 0.6 & 0.1 & 0.2 & 0.1 \\ 0.3 & 0.2 & 0.3 & 0.2 \\ 0.1 & 0.5 & 0.4 & 0 \\ 0 & 0.2 & 0.1 & 0.7 \end{bmatrix}, A_1 = \begin{bmatrix} 0.1 & 0.1 & 0.2 & 0.6 \\ 0.3 & 0.2 & 0.3 & 0.2 \\ 0.4 & 0.2 & 0.4 & 0 \\ 0.2 & 0.5 & 0.1 & 0.2 \end{bmatrix}, \tag{31}$$

Following the procedure outlined above, we can decompose the difference as:

$$\begin{aligned} A_1 &= A_0 + 0.5Z(1, 4; 4, 1) + 0.3Z(3, 4; 3, 4) \\ &= A_0 + 0.5\begin{bmatrix} -1 & 0 & 0 & 1 \\ 0 & 0 & 0 & 0 \\ 0 & 0 & 0 & 0 \\ 1 & 0 & 0 & -1 \end{bmatrix} + 0.3\begin{bmatrix} 0 & 0 & 0 & 0 \\ 0 & 0 & 0 & 0 \\ 1 & -1 & 0 & 0 \\ -1 & 1 & 0 & 0 \end{bmatrix}. \end{aligned} \tag{32}$$

3.2.2 Decompose to a sequence of adjacent mass movements

Now we have the decomposition (28), and the next step is to express any non-adjacent mass movement as a sequence of adjacent mass movements. Suppose that the r^*-th mass movement, $Z\left(i_{r^*}, k_{r^*}; l_{r^*}, j_{r^*}\right)$, in (28) is not an adjacent mass movement. Define the intermediate matrix:

$$\tilde{A}_{r^*-1} := A_0 + \sum_{r=1}^{r^*-1} Z(i_r, k_r; l_r, j_r). \tag{33}$$

The goal is to derive the following decomposition formula:

$$\tilde{A}_{r^*} := \tilde{A}_{r^*-1} + a_{r^*} Z\left(i_{r^*}, k_{r^*}; l_{r^*}, j_{r^*}\right) = \tilde{A}_{r^*-1} + \sum_{s=1}^{R_{r^*}} \beta_{r_s^*} Z\left(i_{r_s^*}, k_{r_s^*}; l_{r_s^*}, j_{r_s^*}\right), \tag{34}$$

where each $Z\left(i_{r_s^*}, k_{r_s^*}; l_{r_s^*}, j_{r_s^*}\right)$ belongs to $\mathcal{B}$, and the intermediate sum $\tilde{A}_{r^*-1} + \sum_{s=1}^{R^0_{r^*}} \beta_{r_s^*} Z\left(i_{r_s^*}, k_{r_s^*}; l_{r_s^*}, j_{r_s^*}\right)$ remains within the checkerboard copula domain at each steps $R^0_{r^*} < R_{r^*}$. Note that the operation of adding $a_{r^*} Z\left(i_{r^*}, k_{r^*}; l_{r^*}, j_{r^*}\right)$ to $\tilde{A}_{r^*-1}$ is equal to the process of transporting a mass a_{r^*} from j^*-th column to l^*-th column in the i^*-th row, and reversely transporting the a same mass from l^*-th column to j^*-th column in the k^*-th row. However, since the j^*-th and l^*-th columns are not adjacent, this process need to be decomposed into a sequence of adjacent mass movements. To achieve this, we leverage the fact that $\tilde{A}_{r^*-1}$ is a checkerboard copula. Specifically, we use the existing mass in certain elements of $\tilde{A}_{r^*-1}$ as an intermediate bridge to facilitate the step-by-step transportation of mass between non-adjacent columns. In particular, to transport a mass from j^*-th column to l^*-th column, we first transport it to its neighboring column which tends to the l^*-th column, such as the (j^*+1)-th column. In this neighbouring transport (from j^*-th to (j^*+1)-th column), we need to keep the immediated matrix as checkerboard copula, which means that we also need to transport a same mass from (j^*+1)-th to j^*-th column. Note that each strictly positive element at position (i, j) can be used to transport at most $\left(\tilde{A}_{r^*-1}\right)_{ij}$ mass out. Therefore, the maximum amount of mass that can be transported from (j^*+1)-th to j^*-th column is limited by the largest element value in the (j^*+1)-th column outside the i^*-th row. We denote this maximum available mass as $\tilde{a}^{i^*}_{j^*+1}$. And note that $\tilde{a}^{i^*}_{j^*+1} > 0$, which follows directly from the properties of checkerboard copula, ensuring that there is always a positive amount of mass available for transport in the intermediate columns. As a result, the amount of mass that can actually be transported from the j^*-th to the (j^*+1)-th columns at the i^*-th row is at most $\min\left\{a_{r^*}, \tilde{a}^{i^*}_{j^*+1}\right\}$. Sequentially, we can transport at most $\min\left\{a_{r^*}, \tilde{a}^{i^*}_{j^*+1}, \tilde{a}^{i^*}_{j^*+1}\right\}$ from the (j^*+1)-th column to the (j^*+2)-th column, then to the (j^*+3)-th column, and so on, until reaching the l^*-th column. The maximum amount of mass that can be transported along this procedure is given by

$$\beta_{r^*} = \min\left\{a_{r^*}, \tilde{a}^{i^*}_{j^*+1}, \ldots, \tilde{a}^{i^*}_{l^*-1}\right\} \tag{35}$$

Similarly, we can transport back the same amount of mass in the reverse direction, from the l^*-th column to the j^*-th column, step by step. This process is equal to add $\beta_{r^*} Z\left(i_{r^*}, k_{r^*}; l_{r^*}, j_{r^*}\right)$ to $\tilde{A}_{r^*-1}$, while ensuring that all intermediate matrices remain within the checkerboard copula domain. If $\beta_{r^*} < a_{r^*}$, meaning that we have only transported part of the required mass, we need repeat the same process iteratively with the remaining mass $a_{r^*} - \beta_{r^*}$ until the entire mass a_{r^*} has been fully transported.

Example 2. To illustrate the above procedure, we continue analyzing Example 1. As seen in the decomposition from (32), the first mass movement step is not adjacent and must be decomposed into a series of adjacent movements. In the first mass movement $A_0 + 0.5Z(1.4;\ 4;\ 1)$, we need to transfer a mass of 0.5 from the 1-st column to the 4-th column in the 1-st row. Since these columns are not adjacent, we can use the 2-nd and 3-rd columns as intermediaries. The maximum mass that can be transported at once is determined by the available mass in these intermediate columns: the 2nd column is at most 0.5, and the 3rd column is at most 0.4. Thus, the largest transferable mass in one step is:

$$\beta_1 = \min\{0.5, 0.5, 0.4\} = 0.4 \tag{36}$$

Accordingly, we first transport 0.4 from the 1st to the 4th column using the 2nd and 3rd columns as bridges in the 1st row, and an equal amount is transported in reverse along the 4th row. After this step, there is 0.1 mass left to be transported, which we handle by repeating the same process. The final decomposition is given by:

$$\begin{aligned} A_0 + 0.5Z(1,4;4,1) = A_0 &+ 0.4[Z(1,3;2,1) + Z(1,3;3,2) + Z(1,4;4,3) + Z(3,4;3,2) + Z(3,4;2,1)] \\ &+ 0.1[Z(1,3;2,1) + Z(1,3;3,2) + Z(1,4;4,3) + Z(3,4;3,2) + Z(3,4;2,1)]. \end{aligned} \tag{37}$$

We have now constructed a continuous interpolation between A_0 and A_1, and proceed to analyze the associated transport effort. In the decomposition of each non-adjacent mass movement $a_{r^*}Z\big(i_{r^*}, k_{r^*}; l_{r^*}, j_{r^*}\big)$ in (28), the mass must be transported from the j^*-th column to l^*-th column and then returned. The number of adjacent transport steps involved is at most $2\big|l^* - j^*\big| < 2N$, which implies that the transport effort for the single basic movement is bounded by $2N * 2a_{r^*}/N$. Since there are at most $R \le N^4$ basic mass movements and each coefficient satisfies $a_{r^*} \le 2^R \big\|A_1 - A_0\big\|_{\max}$, the total transport effort of the interpolation is bounded by

$$\text{Transport effort} \le \sum_{r^*=1}^{R} \frac{2N * 2a_{r^*}}{N} \le \sum_{r^*=1}^{R} 4 \cdot 2^R \big\|A_1 - A_0\big\|_{\max} \le 4 \cdot 2^{N^4} N^4 \big\|A_1 - A_0\big\|_{\max}. \tag{38}$$

This bound is extremely loose, as it is derived by taking the worst-case estimates throughout the construction. Nevertheless, it shows that the transport effort tends to zero as $\big\|A_1 - A_0\big\|_{\max} \to 0$.

3.2.3 Example: Gaussian copula and Gumbel copula

Now, we illustrate the constructed continuous interpolation using checkerboard copulas derived from Gaussian copula and Gumbel copula as an example. Consider two copulas C_0 and C_1, where C_0 is the Gaussian copula with correlation parameter $\rho = 0.8$, and C_1 is the Gumbel copula with parameter $\theta = 2.3$. Their corresponding checkerboard copulas, denoted by A_0 and A_1, are obtained via the equation (7), with $N = 20$. Using the constructed continuous interpolation method, A_0 and A_1 can be connected through $I = 5{,}570$ adjacent mass-movement steps. The total transport effort associate with this interpolation is 1.337.

To illustrate the behavior of this interpolation in terms of transport effort, we parameterize the interpolation path from A_0 to A_1 using transport effort as the x-axis. Specifically, the interval [0, 1] is divided into 100 subintervals, each corresponding to an equal amount of transport effort. Figure 2 shows the interpolated copulas at effort levels corresponding to 0, 0.2, 0.4, 0.6, 0.8, 1 of the total transport effort, respectively. In this figure, small bumps appear along the edges because, in our row-by-row construction, particles with larger mass are transferred to cells with smaller mass.

Figure 3 (left) presents the Kendall's τ and Spearman's ρ of the interpolated copulas, where τ and ρ are computed using the formulas (10). As shown in the figure, both dependence measures, ρ and τ, do not exhibit drastic changes in the equal-effort steps, thereby reflecting a certain degree of "continuity" in this interpolation. However, their evolution is not monotonic, which is undesirable from the viewpoint of constructing a well-behaved interpolation path.

If we treat checkerboard copulas as their corresponding discrete measures according to (16), the Wasserstein distance between two checkerboard copulas can be computed using an optimal transport (OT) solver (Bonneel et al. 2011) via the network simplex algorithm, as implemented in the POT library (Flamary et al. 2021). Figure 3 (right) shows the Wasserstein distances W_1 and W_2 between the interpolated copulas and both the initial copula A_0 and the target copula A_1. In this figure, both Wasserstein distance curves exhibit noticeable irregularities, which is consistent with our construction, since the Wasserstein distance was not taken into account during the process. Additionally, we find that $W_1(A_0, A_1) = 0.3071$, which is smaller than Transport effort $= 1.3271$, aligning with the relationship (25).

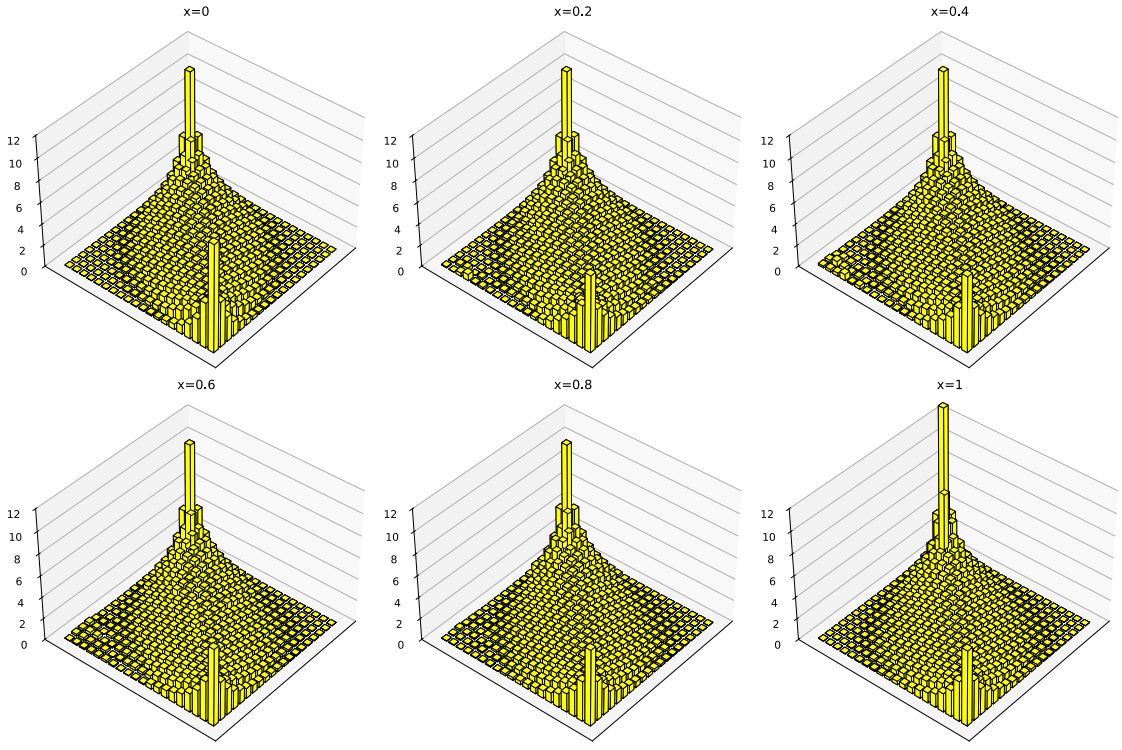

Figure 2: The interpolated checkerboard copulas at different transport efforts. *Z*-axis represent the density of copula.

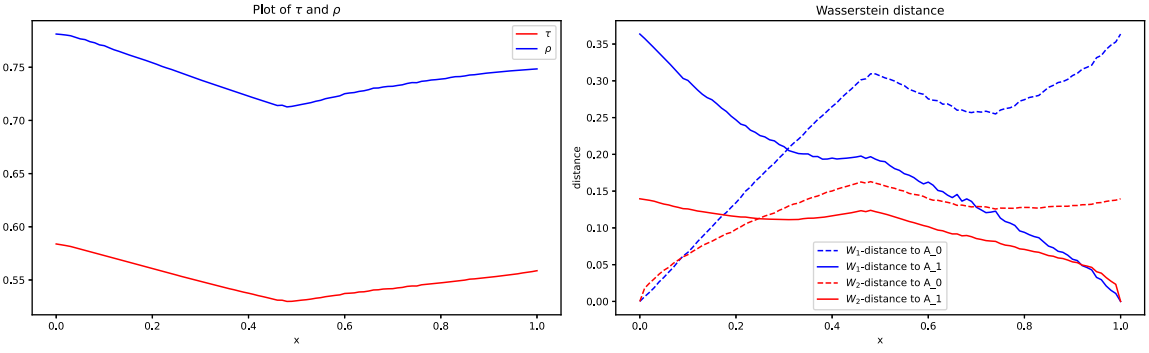

Figure 3: Left: Kendall's τ and Spearman's ρ in the continuous interpolation. Right: Wasserstein distance W_1 and W_2 between the interpolated copulas and the initial A_0 and target A_1, respectively.

3.3 High dimensional case

We now outline the multivariate extension. Similar to the two-dimensional case, the set of d-dimensional checkerboard copulas has a one-to-one correspondence with the set of d-plane-stochastic tensors, defined as

$$S_N^d = \left\{ A \in \mathbb{R}^d : A_{i_1 i_2 \dots i_d} \geq 0, \quad \sum_{i_1,\dots,i_{j-1},i_{j+1},\dots,i_d} A_{i_1 i_2 \dots i_d} = 1 \quad \text{for } \forall j \in \{1,2,\dots,d\} \right\}. \tag{39}$$

The correspondence between a checkerboard copula C and a tensor A is given by

$$A_{i_1\dots i_d} = N\sum_{K=0}^{d}\sum_{\{j_1,\dots,j_K\}\subset\{1,\dots,d\}}(-1)^K C_{i_1,\dots,i_{j_1}-1,\dots,i_{j_K}-1,\dots,i_d}, \tag{40}$$

For example, when $d = 3$, the relationship formula is

$$\begin{aligned} A_{ijk} = N\big(&C_{i,j,k} - C_{i-1,j,k} - C_{i,j-1,k} - C_{i,j,k-1} + C_{i-1,j-1,k} \\ &+ C_{i-1,j,k-1} + C_{i,j-1,k-1} - C_{i-1,j-1,k-1}\big). \end{aligned} \tag{41}$$

Although, to the best of our knowledge, there is no convex combination representation analogous to the Birkhoff–von Neumann theorem for d-plane stochastic tensors when $d \geq 3$, it is still possible to construct a continuous interpolation path. The construction idea is similar to that of the two-dimensional case. In this setting, the basic adjacent mass-movement is represented by an integer tensor $Z = Z(k_1, \dots, k_d, l_1, \dots, l_d;\ j)$, defined as

$$Z_{i_1\dots i_d} = \begin{cases} -1 & (i_1,\dots,i_d) = (k_1,\dots,k_d),(l_1,\dots,l_d), \\ +1 & (i_1,\dots,i_d) = (k_1,\dots,k_{j-1},l_j,k_{j+1},\dots k_d),(l_1,\dots,l_{j-1},k_j,l_{j+1},\dots,l_d), \\ 0 & \text{otherwise.} \end{cases} \tag{42}$$

where $\left|k_j - l_j\right| = 1$. Adding aZ to a checkerboard copula A corresponds to transferring a small amount of mass from the cells $(k_1, \dots, k_d)$ and $(l_1, \dots, l_d)$ to $(k_1, \dots, k_{j-1}, l_j, k_{j+1}, \dots, k_d)$ and $(l_1, \dots, l_{j-1}, k_j, l_{j+1}, \dots, l_d)$ respectively, along the j-th axis. This operation is evidently adjacent in the tensor grid.

With the adjacent mass movement defined above, we can construct a continuous interpolation in a manner similar to that in the previous section. The construction proceeds plane by plane along the d-th axis. We begin with the plane $i_d = 1$, where mass is gradually adjusted until the two copulas coincide on this layer, before moving on to the next plane. More precisely, let $Z = A_1 - A_0$, and start with the plane $i_d = 1$. We identify the elements of Z with the minimum and maximum values within this plane, denoted by $(i_1, \dots, i_{d-1}, 1)$ and $\left(i'_1, \dots, i'_{d-1}, 1\right)$, respectively. We then need to move the corresponding mass of A_0 from cell $(i_1, \dots, i_{d-1}, 1)$ to $\left(i'_1, \dots, i'_{d-1}, 1\right)$. This movement is achieved sequentially along the coordinate axes: we first transfer mass from $(i_1, \dots, i_{d-1}, 1)$ to $\left(i'_1, i_2, \dots, i_{d-1}, 1\right)$, then to $\left(i'_1, i'_2, i_3, \dots, i_{d-1}, 1\right)$, and so on, until we reach $\left(i'_1, \dots, i'_{d-1}, 1\right)$ along the 1st, 2nd, …, and $d-1$-th axes, respectively. The detailed construction follows the same principle as in the two-dimensional case. The total number of steps required is less than $2^{d-1}N^{3d-2}$. As an illustration, we provide an example of a three-dimensional checkerboard copula in the Appendix.

4 Interpolation path induced by optimal transport

To obtain a more direct interpolation, we aim to follow the structure of the displacement interpolation, which corresponds to the shortest path with respect to the Wasserstein distance (Section 4.1). Since this path generally lies outside the copula domain, we construct a copula grid by discretizing the displacement interpolation into a sequence of intermediate measures, and then mapping them into checkerboard copulas via the inverse of Sklar's theorem (Section 4.2). This grid of copulas lies close to the displacement path in Wasserstein space. To stay within the copula domain while preserving continuity, we then connect adjacent grid points sequencely, using the previously introduced continuous interpolation. The resulting path remains entirely within the copula domain and closely follows the true Wasserstein geodesic; we refer to it as a displacement-like interpolation. In what follows, we focus on the geodesic in the Wasserstein-2 space.

4.1 Displacement interpolation

The displacement interpolation, for two checkerboard copulas A_0 and A_1 with densities f_0 and f_1 expressed by the formula (9), is the solution of dynamical optimal transport problem (12) with $\Omega = [0,1]^2$. To solve this problem, appropriate boundary conditions need to be considered. In this study, we use homogeneous Neumann conditions: $v(t,x)|_{\partial\Omega} = 0$, which in our case means that the mass cannot flow across the boundary of the unit square and hence the total (probability) mass in Ω is conserved.

Note that the dynamical optimal transport problem (12) is not convex in the variables (f, v), as the continuity equation involves the product fv. Introducing the change of variables $(f, v) \mapsto (f, m)$ where $m = fv$ is the momentum, it becomes convex as follows:

$$\begin{aligned} &\min_{(f,m)\in C} \int_0^1 \int_{[0,1]^2} J(f(t,x), m(t,x))\mathrm{d}x\mathrm{d}t, \\ &C = \{(f,m)\colon \partial_t f + \mathrm{div}_x m = 0,\ f(0,\cdot,\cdot) = f_0,\ f(1,\cdot,\cdot) = f_1, m(t,x)|_{\partial\Omega} = 0\}, \end{aligned} \tag{43}$$

where $J\colon \mathbb{R}\times\mathbb{R}^2 \to \mathbb{R}^+ \cup \{+\infty\}$ is the following lower semicontinuous convex function,

$$J(f,m) = \begin{cases} \dfrac{|m|^2}{2f} & \text{if } f > 0, \\ 0 & \text{if } f = 0, \\ +\infty & \text{otherwise.} \end{cases} \tag{44}$$

We discretize the time as $t_k = \frac{2k-1}{2Q}$ where $k = 1, 2, \dots, Q$, and assume the space is uniformly discretized at points $(\frac{2i-1}{2N}, \frac{2j-1}{2N})$ where $i, j = 1, 2, \dots, N$, in order to be consistent with checkerboard copula, i.e., the points address the centers of the checkerboard cells in (9). Using a staggered grid representation which is commonly used in fluid dynamics, the path $f(t,x)$ is represented by $\mathbf{f} \in \mathbb{R}^{(Q+1)\times N\times N}$ associated to the grid points $\{i/Q\}_{i=0,1,\dots,Q}$ in time, and the momentum $m = (m^1, m^2)$ is represented by $\mathbf{m} = (\mathbf{m}^1, \mathbf{m}^2)$ where $\mathbf{m}^1 \in \mathbb{R}^{Q\times(N+1)\times N}$ and $\mathbf{m}^2 \in \mathbb{R}^{Q\times N\times(N+1)}$ are associated to half grid points in each space direction. Then a discrete counterpart to the continuity equation is

$$(\partial_t \mathbf{f} + \mathrm{div}_x \mathbf{m})_{kij} = Q(\mathbf{f}_{k,i,j} - \mathbf{f}_{k-1,i,j}) + N\Big(\mathbf{m}^1_{k,i,j} - \mathbf{m}^1_{k,i-1,j}\Big) + N\Big(\mathbf{m}^2_{k,i,j} - \mathbf{m}^2_{k,i,j-1}\Big), \tag{45}$$

and the constraint set in (43) is

$$\mathbf{C} = \Big\{(\mathbf{f},\mathbf{m})\colon \partial_t \mathbf{f} + \mathrm{div}_x \mathbf{m} = 0, \mathbf{f}_{0ij} = (f_0)_{ij}, \mathbf{f}_{Qij} = (f_1)_{ij}, \mathbf{m}^1_{k0j} = \mathbf{m}^1_{kNj} = \mathbf{m}^2_{ki0} = \mathbf{m}^2_{kiN} = 0\Big\}. \tag{46}$$

For the discretization of the function (f, m) in (43), we use the midpoint interpolation operator $\mathcal{I}$, defined as follows:

$$\forall 1 \le k \le Q, \quad \forall 1 \le i,j \le N, \quad \begin{cases} f_{kij} = (\mathbf{f}_{k,i,j} + \mathbf{f}_{k,i-1,j})/2, \\ m^1_{kij} = \Big(\mathbf{m}^1_{k,i,j} + \mathbf{m}^1_{k,i-1,j}\Big)/2, \\ m^2_{kij} = \Big(\mathbf{m}^2_{k,i,j} + \mathbf{m}^2_{k,i,j-1}\Big)/2. \end{cases} \tag{47}$$

Now the discretization of continuous problem (43) is a finite dimensional convex problem,

$$\min_U \mathcal{J}(\mathcal{I}(U)) + \iota_{\mathbf{C}}(U), \tag{48}$$

where $U = (\mathbf{f}, \mathbf{m})$ and

$$\mathcal{J}(\mathcal{I}(U)) := \sum_{i,j=1}^{N}\sum_{k=1}^{Q} J(f_{kij}, m_{kij}), \tag{49}$$

and $\iota_{\mathbf{C}}$ is the indicator function of the closed convex set $\mathbf{C}$,

$$\iota_{\mathbf{C}}(U) = \begin{cases} 0 & \text{if } U \in \mathbf{C}, \\ +\infty & \text{otherwise.} \end{cases} \tag{50}$$

Note that $\mathcal{J}$ and $\iota_{\mathbf{C}}$ are both lower-semicontinuous convex function, and $\mathcal{I}$ is linear. Therefore, we can use a first-order primal-dual algorithm to solve the discrete problem (48), by computing a sequence $(U^n, V^n, \bar{U}^n)$ according to

$$\begin{aligned} V^{n+1} &= \mathrm{Prox}_{\sigma\mathcal{J}^*}\left(V^n + \sigma\mathcal{I}\bar{U}^n\right), \\ U^{n+1} &= \mathrm{Prox}_{\tau\iota_{\mathbf{C}}}\left(U^n - \tau\mathcal{I}^* V^{n+1}\right), \\ \bar{U}^{n+1} &= 2U^{n+1} - U^n, \end{aligned} \tag{51}$$

where $\tau\sigma\|\mathcal{I}\|^2 < 1$, and the proximal operator for a convex function F is defined as

$$\mathrm{Prox}_{\sigma F}(y) = \arg\min_x F(x) + \frac{\|x-y\|^2}{2\sigma}, \quad \text{for } \sigma > 0. \tag{52}$$

The proximal operator $\mathrm{Prox}_{\sigma\mathcal{J}^*}$ is computed by solving a cubic polynomial equation, while $\mathrm{Prox}_{\tau\iota_{\mathbf{C}}}$ is a linear projector, computed via the inversion of a linear system. The convergence proof for this algorithm can be found in Chambolle and Pock (2011), and we refer to paper (Papadakis et al. (2014) for detailed discussion and computation.

In the above algorithm, we ultimately obtain a sequence $U_n = (\mathbf{f}_n, \mathbf{m}_n)$, where U_n is a convergent sequence, and we assume that $U_n \to U^* = (\mathbf{f}, \mathbf{m})$. Here, $\mathbf{f} \in \mathbb{R}^{(Q+1)\times N\times N}$ represents the desired displacement interpolation between f_0 and f_1 at times $0, 1/Q, 2/Q, \dots, 1$. However, these are not in the copula domain. To address this, we will use Sklar's theorem, which establishes the connection between a distribution and its corresponding copula, to obtain the copulas associated with $\mathbf{f}$.

4.2 Inverse statement of Sklar's theorem

According to the inverse statement of Sklar's theorem, the copula $C(u, v)$ corresponding to a given joint distribution $F(x, y)$ can be expressed as the composition of the distribution $F(x, y)$ and the quantile functions of its marginal distributions, F_X^{-1} and F_Y^{-1}:

$$C(u, v) = F\left(F_X^{(-1)}(u), F_Y^{(-1)}(v)\right) \quad \text{for} \quad (u, v) \in [0, 1]^2. \tag{53}$$

Assume that the domain of F is the unit square, and the density f is uniformly distributed as follows:

$$f(x, y) = f_{ij} \quad \text{for} \quad (x, y) \in \left(\frac{i-1}{N}, \frac{i}{N}\right] \times \left(\frac{j-1}{N}, \frac{j}{N}\right]. \tag{54}$$

Under this assumption, the densities of the marginal distributions of F are piecewise constant. Specifically, $f_X(x) = \sum_{k=0}^N f_{ik}/N$ and $f_Y(y) = \sum_{k=0}^N f_{ki}/N$ for $x, y \in (\frac{i-1}{N}, \frac{i}{N}]$. As a result, the marginal distributions are both piecewise linear functions on the interval [0, 1], and their quantile functions F_X^{-1}, F_Y^{-1}, are also piecewise linear and can be explicitly determined. Consequently, the corresponding copula can be explicitly computed using formula (53).

The displacement interpolation $\mathbf{f} \in \mathbb{R}^{(Q+1)\times N\times N}$, derived in the previous subsection, is a sequence of $Q+1$ ordered distributions whose density can be expressed using formula (54). This allows the explicit computation of the copula $\mathbf{A}_k$ corresponding to each interpolated density $\mathbf{f}_k$ at discrete times $t_k = k/Q$. By transforming each interpolated density $\mathbf{f}_k$ into its corresponding copula, we construct an ordered sequence of copulas $\mathbf{A}_k$, $k = 0, 1, 2, \dots, Q$. At $t = 0$, the initial interpolation $\mathbf{f}_0$ corresponds to the discretization of the initial density f_0, which is associated with the initial checkerboard copula A_0. Therefore, $\mathbf{A}_0 = A_0$. Similarly, at $t = 1$, the final interpolation $\mathbf{f}_Q$ corresponds to the final checkerboard copula A_1, so $\mathbf{A}_Q = A_1$. Thus, the ordered sequence of $Q+1$ matrices $\mathbf{A}_k$ effectively represents an interpolation between A_0 and A_1 at discrete times $t_k \in \{0, 1/Q, \dots, 1\}$, as induced by the dynamical optimal transport.

Since this interpolation is based on the Wasserstein distance, the W_2-distance can be used to analyze how far the induced interpolation $\mathbf{A}_k$ is from the displacement interpolation $\mathbf{f}_k$. In general, they are very close in terms of the W_2-distance (see the detailed illustration in the example provided in the next section). From this perspective, the induced interpolated copula $\mathbf{A}_k$ can be regarded as nearly optimal with respect to the W_2-distance.

5 Application

In this section, we illustrate the final displacement-like interpolation by sequentially connecting the grid of copulas constructed as in Section 4 along the W_2 geodesic, using the continuous interpolation introduced in Section 3. In this interpolation, each step corresponds to an adjacent mass movement, and the entire path remains close to the true geodesic between the initial and final checkerboard copulas in the Wasserstein-2 space. To demonstrate the behavior and advantages of this combined approach, we present two examples: a toy example and a practical example. The three-dimensional case is further illustrated in the Appendix. The implementation code is available at *github.com/Interpolation-checkerboard-copula*.

5.1 Toy example: checkerboard copula from Gaussian copula and Gumbel copula

We use the checkerboard copulas A_0 and A_1 in the example in Section 3.2.3 to demonstrate the displacement-like interpolation. Taking $Q = 20$, the interpolated copula $\mathbf{A}_k$, induced by optimal transport at different times, is shown in Figure 4. From this figure, we observe that the copula evolves continuously and smoothly to some extent along the interpolation process from a whole perspective. Next, we connect these copulas $\mathbf{A}_k$ sequentially by adjacent mass movements to obtain the final displacement-like interpolation. In this case, connecting A_0 and A_1 requires a total of $I = 228,094$ adjacent mass-movement steps, with an overall transport effort of 1.370.

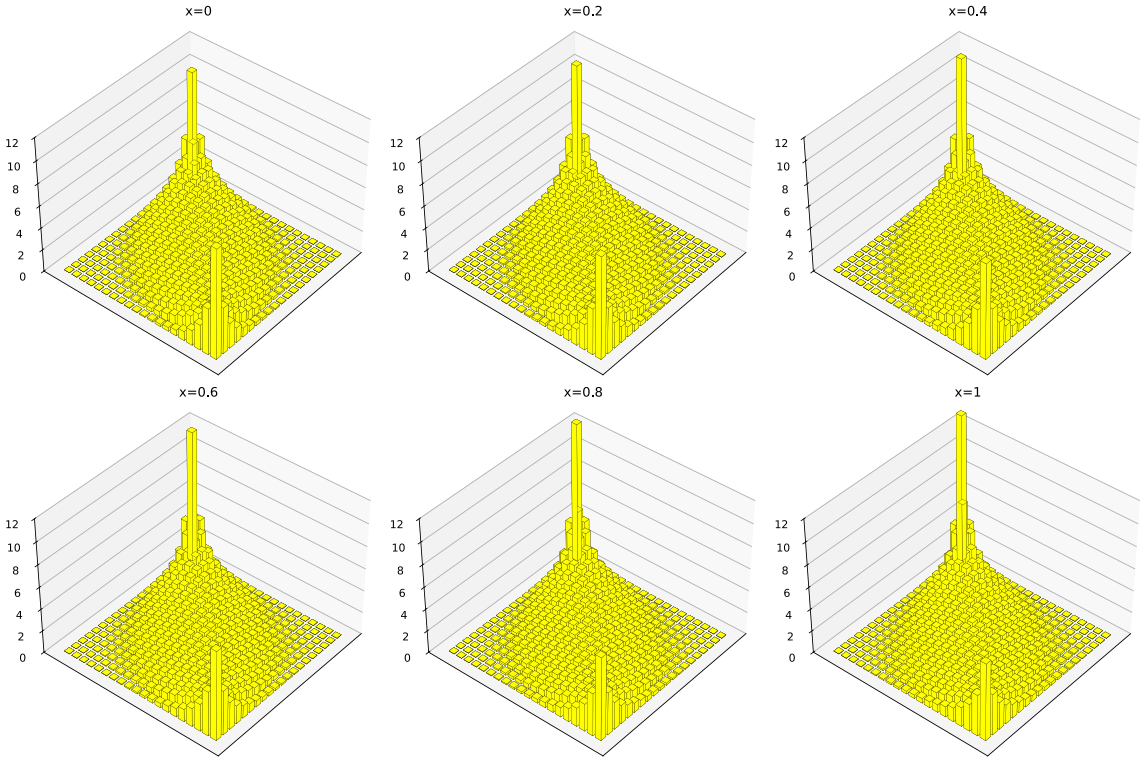

Figure 4: The interpolation between the two checkerboard copulas A_0 and A_1 induced by the dynamical optimal transport at different transport efforts.

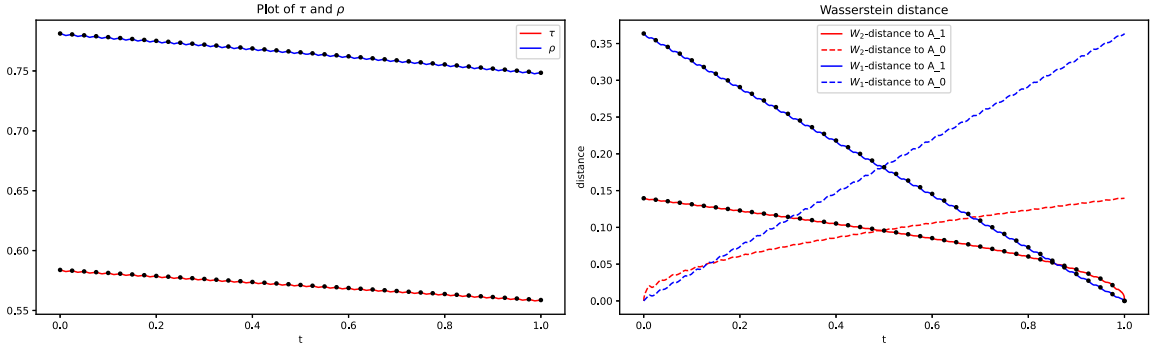

Figure 5: The displacement-like interpolation between the two checkerboard copulas A_0 and A_1. Left: τ and ρ. Right: Wasserstein distance.

Compared to the continuous interpolation in Example 3.2.3, the number of adjacent mass-movement steps has increased substantially. This is expected, as we are now connecting $Q+1$ intermediate copulas sequentially. Despite the significant increase in the number of steps, the growth in transport effort remains relatively modest.

To analyze the behavior of this displacement-like interpolation, we plot the Kendall's τ and Spearman's ρ values of the copulas along the evolution, as shown in Figure 5 (left). In this figure, the black dots represent the τ and ρ of the $Q+1$ interpolated copulas induced by optimal transport. From this figure, we observe that both τ and ρ exhibit a stronger continuity and monotonicity compared with that in Example 3.2.3. From this perspective, the interpolation can be regarded as a well-behaved evolution between the initial τ (or ρ) and the final τ (or ρ). This property is not limited to this specific case. In general, the interpolation between any two checkerboard copulas obtained from the discretization of Gaussian, Clayton, Gumbel, Frank, or Independence copulas demonstrates continuous and monotonic evolution of τ and ρ from their initial to final values. Consequently, this interpolation has significant potential as a tool for modeling the evolution of dependence measures τ and ρ.

Figure 5 (right) represents the W_1- and W_2-distances between the interpolated copulas and both the initial copula A_0 and target A_1. The black dots denote the Wasserstein distances between the $Q+1$ distributions on the displacement interpolation path and the target copula A_1. These points lie almost in a straight line in the case W_2, and the lines that describe W_2-distances exhibit an approximate symmetry with respect to $t=0.5$; This is consistent with the fact that displacement interpolation follows a constant-speed geodesic connecting the initial and final measures. From this figure, we observe that the red line closely follows the black dots, indicating that the displacement-like interpolation closely approximates the optimal transport path. This proximity reflects a degree of optimality in this interpolation, aligning it to some extent with the principles of optimal transport.

5.2 Practical example

In this section, we illustrate the displacement-like interpolation using an example from Coblenz et al. (2020). In that paper, the authors model the distribution of fuel droplet sizes generated by a fuel injector in a jet engine using vine copulas, and generate realistic samples under different operating conditions based on the learned model. By analyzing data across various jet engine settings, they calibrate a model with eight parameters that are applicable to all conditions. To handle scenarios with missing data, they suggest to interpolate the model parameters. In contrast, we interpolate the data on known operating conditions directly using displacement-like interpolation.

We use the data sets 50-1-640 and 90-1-640, where "50-1-640" represents the operating condition: air velocity $=50\ \mathrm{ms}^{-1}$, air pressure $=1$ bar, thickness of atomizing edge $=640\ \mu$m, and "90-1-640" is similar. We focus on interpolating the data for the variables y-position and x-velocity, which are modeled by a U-shaped copula obtained by gluing a t-copula and a Joe copula. We first take the pseudo-observations of the data, and then compute their histograms on the uniform division $I_N \times I_N$ of $[0,1]^2$, where $N=20$. Consequently, we

obtain their corresponding checkerboard copulas denoted as A_0 and A_1, which describe the relationship between y-position and x-velocity for the conditions 50-1-640 and 90-1-640 respectively.

Setting $Q = 20$, the interpolated copulas and the corresponding plots of Kendall's τ, Spearman's ρ, and the relevant Wasserstein distance are shown in Figures 6 and 7. The number of adjacent mass-movement steps is 83,587, and the transport effort is 4.533. As shown in Figure 6, the shape of the interpolated copulas evolves gradually while consistently preserving a U-shaped structure, even though the available dataset contains only 1,240 points.

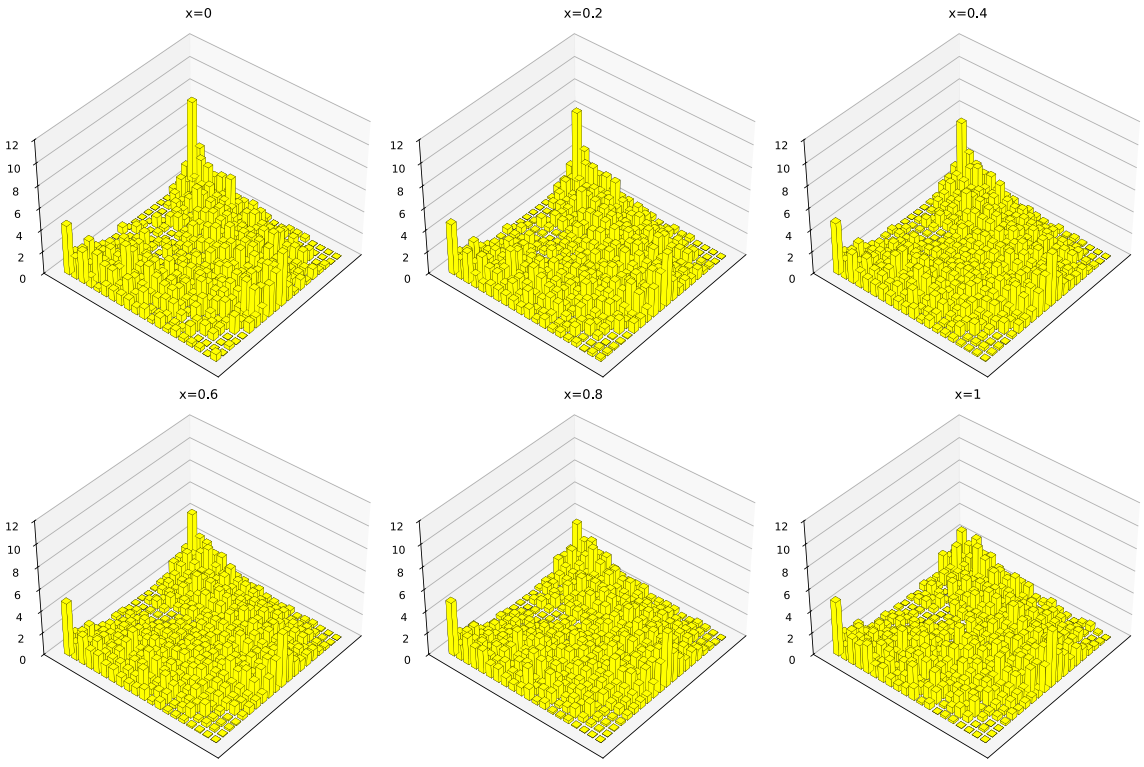

Figure 6: The interpolation between the data sets on conditions 50-1-640 and 90-1-640.

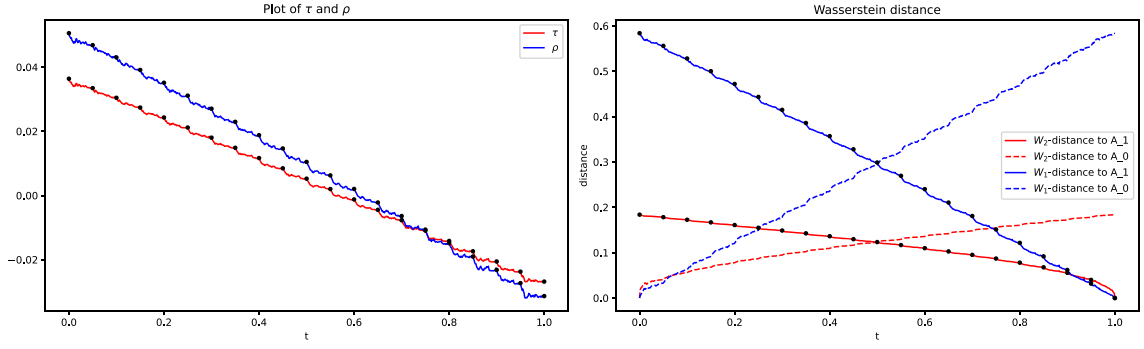

Figure 7: The displacement-like interpolation between the data sets on conditions 50-1-640 and 90-1-640. Left: τ and ρ. Right: Wasserstein distance.

6 Conclusion and discussion

In this work, we present a continuous displacement-like interpolation method between any two given checkerboard copulas, where each step involves an adjacent mass movement. The interpolation closely approximates the geodesic in the Wasserstein-2 space, capturing the smooth and continuous evolution of the copula model from a global perspective. Extending this displacement-like interpolation to the general copula case is an interesting and promising direction. However, such an extension is not straightforward, as the inverse of Sklar's theorem becomes considerably more complex in the general setting.

Moreover, identifying a direct displacement interpolation within the copula domain itself remains a broader and more challenging problem – equivalently, this corresponds to finding an optimal transport path constrained within the copula domain. Research on optimal transport between copulas remains very limited, possibly because the uniform-marginal constraint of copulas makes it challenging to define transport maps or plans that stay within the copula domain.

Acknowledgements: The authors are grateful to the valuable comments of two reviewers that improved the manuscript.
Funding information: Na Luo received financial support provided by the China Scholarship Council (CSC).
Author contributions: Both authors have accepted responsibility for the entire content of this manuscript and consented to its submission to the journal, reviewed all the results, and approved the final version of the manuscript. OG: conceptualization, methodology, writing, supervision. NL: conceptualization, methodology, writing, software, simulation.
Conflict of interest: The authors declare no conflicts of interest related to this publication.

Appendix A

In this appendix, we present the interpolation results between two three-dimensional checkerboard copulas. Specifically, we consider two Gaussian copulas C_0 and C_1 with correlation matrices Σ_0 and Σ_1, given by

$$\Sigma_0 = \begin{bmatrix} 1 & 0.2 & 0.4 \\ 0.2 & 1 & 0.6 \\ 0.4 & 0.6 & 1 \end{bmatrix}, \quad \Sigma_1 = \begin{bmatrix} 1 & -0.2 & 0.8 \\ -0.2 & 1 & 0.1 \\ 0.8 & 0.1 & 1 \end{bmatrix}. \tag{55}$$

The corresponding checkerboard copulas are denoted by A_0^{20}, A_1^{20} and A_0^5, A_1^5 with $N = 20, 5$ respectively.

For $N = 20$, Figures 8 and 9 illustrate the interpolations without and with the optimal transport constraint, respectively. In each figure, for a fixed transport effort ($x =$ constant), the three panels from left to right display the densities of the bivariate margins f_{12}, f_{13} and f_{23}. These results show that the interpolation induced by the dynamical optimal transport path produces smoother transitions across all two-dimensional margins compared with the direct interpolation.

For $N = 5$, Figure 10 shows the Wasserstein distance along the continuous interpolation (Figure 10(a)) and that induced by optimal transport (Figure 10(b)). From this figure, we observe that the Wasserstein distance curve obtained from the optimal transport–based interpolation exhibits better continuity and monotonicity, which is consistent with our expectation.

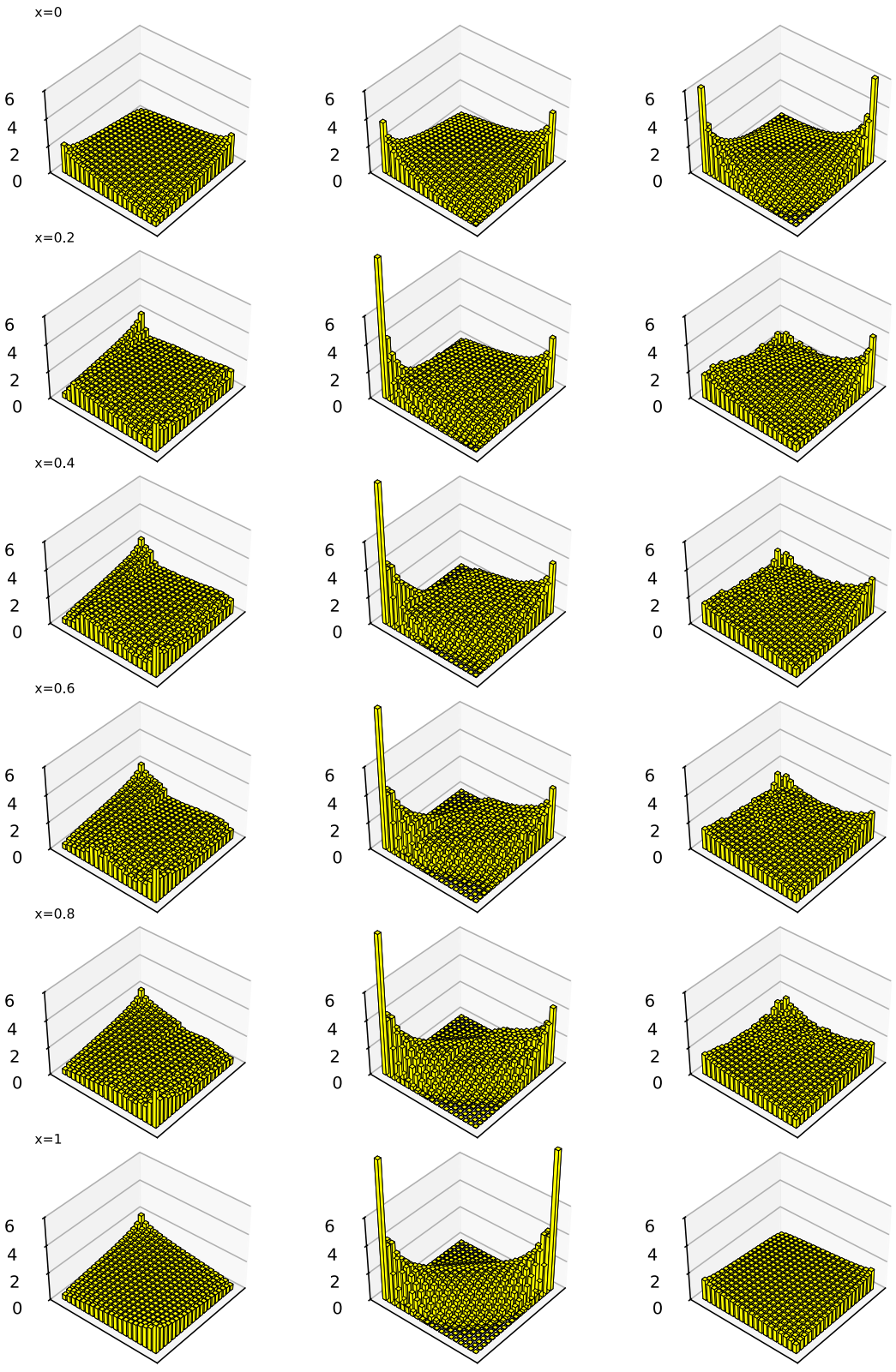

Figure 8: The continuous interpolation between A_0^{20} and A_1^{20}.

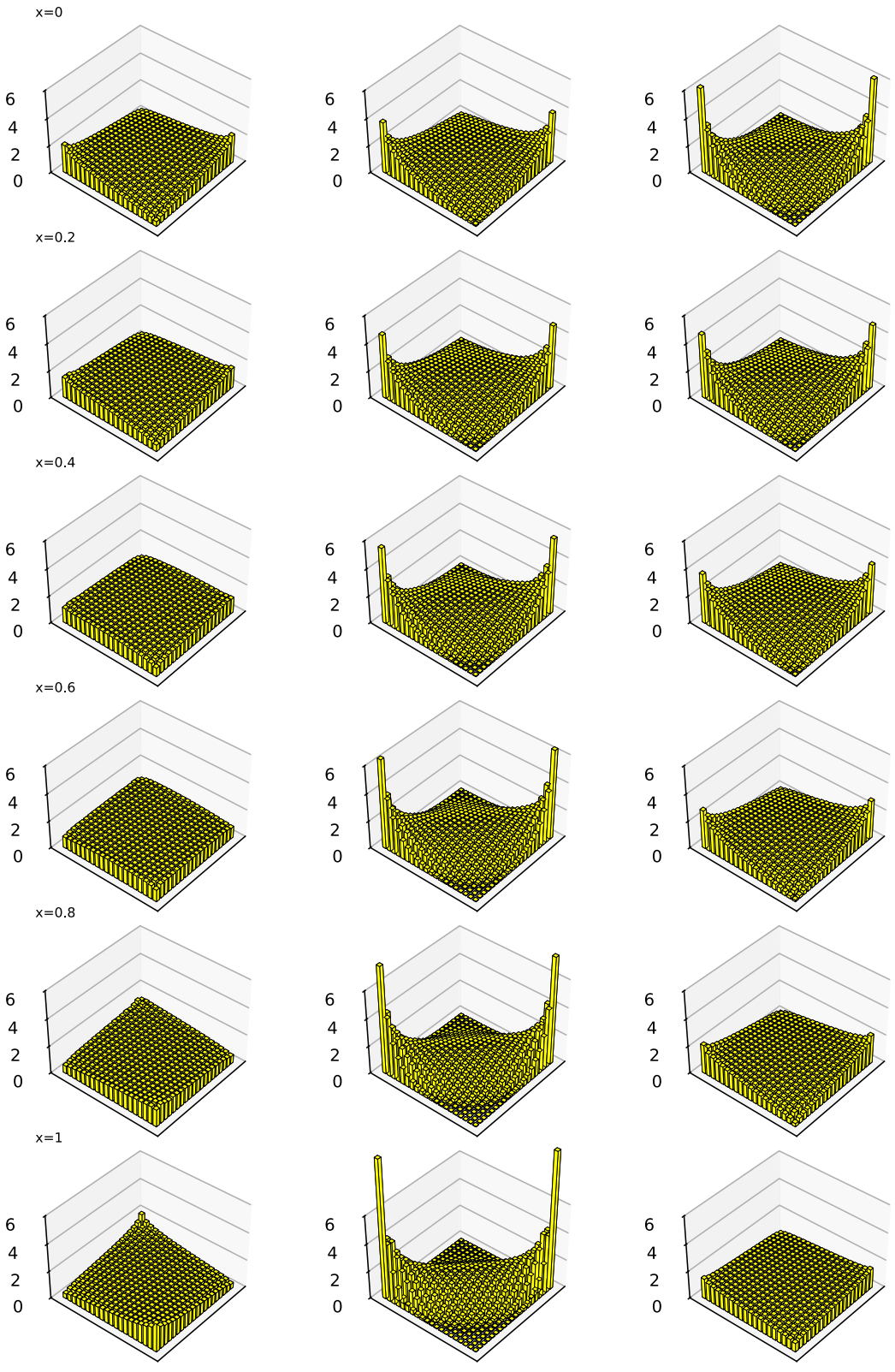

Figure 9: The displacement-like interpolation between A_0^{20} and A_1^{20}.

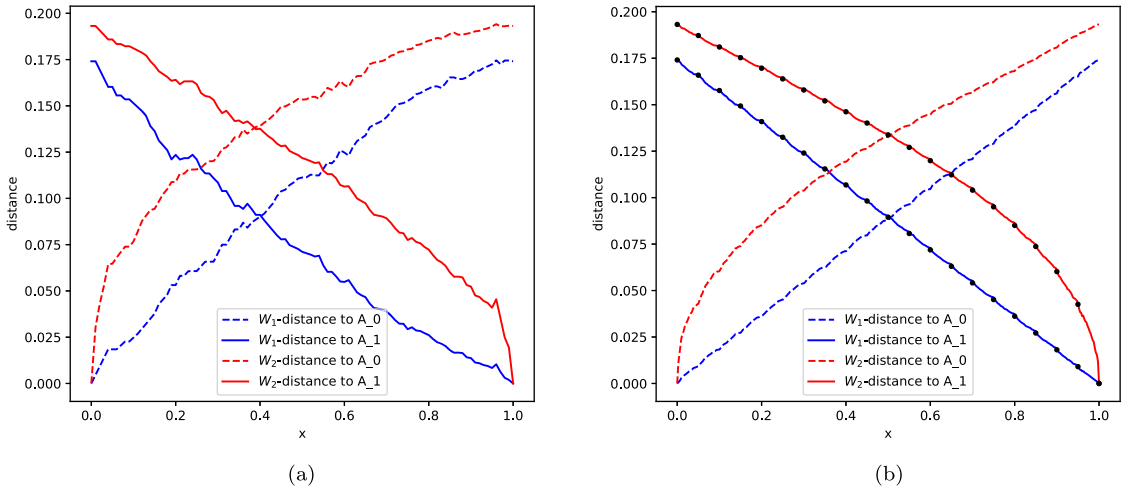

Figure 10: The Wasserstein distance along the interpolations between A_0^5 and A_1^5. (a) Continuous interpolation, (b) displacement-like interpolation.

References

Alfonsi, A. and Jourdain, B. (2014). A remark on the optimal transport between two probability measures sharing the same copula. *Stat. Probab. Lett.* 84: 131—134.

Aoki, S., Hara, H., and Takemura, A. (2012). *Markov bases in algebraic statistics*, 199. Springer Science & Business Media, New York, NY, USA.

Benamou, J.-D. and Brenier, Y. (2000). A computational fluid mechanics solution to the monge-Kantorovich mass transfer problem. *Numer. Math.* 84: 375—393.

Birkhoff, G. (1946). Tres observaciones sobre el algebra lineal. *Univ. Nac. Tucuman, Ser. A* 5: 147—154.

Bonneel, N., Van De Panne, M., Paris, S., and Heidrich, W. (2011). Displacement interpolation using lagrangian mass transport. In: *Proceedings of the 2011 SIGGRAPH Asia conference*, pp. 1—12.

Chambolle, A. and Pock, T. (2011). A first-order primal-dual algorithm for convex problems with applications to imaging. *J. Math. Imag. Vis.* 40: 120—145.

Cherubini, U., Luciano, E., and Vecchiato, W. (2004). *Copula methods in finance*. John Wiley & Sons, Hoboken, NJ, USA.

Chi, J., Ouyang, J., Li, X., Wang, Y., and Wang, M. (2019). Approximate optimal transport for continuous densities with copulas. In: *IJCAI*, pp. 2165—2171.

Chi, J., Wang, B., Chen, H., Zhang, L., Li, X., and Ouyang, J. (2022). Approximate continuous optimal transport with copulas. *Int. J. Intell. Syst.* 37: 5354—5380.

Coblenz, M., Holz, S., Bauer, H.-J., Grothe, O., and Koch, R. (2020). Modelling fuel injector spray characteristics in jet engines by using vine copulas. *J. Roy. Stat. Soc. C Appl. Stat.* 69: 863—886.

Cong, R.-G. and Brady, M. (2012). The interdependence between rainfall and temperature: copula analyses. *Sci. World J.* 2012: 405675—11.

Durante, F. and Sempi, C. (2016). *Principles of copula theory*, 474. CRC Press, Boca Raton, FL.

Durrleman, V., Nikeghbali, A., and Roncalli, T. (2000). Copulas approximation and new families, *Available at SSRN 1032547*.

Flamary, R., Courty, N., Gramfort, A., Alaya, M. Z., Boisbunon, A., Chambon, S., Chapel, L., Corenflos, A., Fatras, K., Fournier, N., et al. (2021). Pot: Python optimal transport. *J. Mach. Learn. Res.* 22: 1—8.

Genest, C., Gendron, M., and Bourdeau-Brien, M. (2009). The advent of copulas in finance. *Eur. J. Fin.* 15, https://doi.org/10.1080/13518470802604457.

Ghaffari, N. and Walker, S. (2021). Parseval's identity and optimal transport maps. *Stat. Probab. Lett.* 170: 108989.

Grothe, O. and Rieger, J. (2024). Decomposition and graphical correspondence analysis of checkerboard copulas. *Depend. Model.* 12: 20240006.

Grothe, O., Schnieders, J., and Segers, J. (2014). Measuring association and dependence between random vectors. *J. Multivariate Anal.* 123: 96—110.

Joe, H. (2014). *Dependence modeling with copulas*. Chapman & Hall/CRC, New York, NY, USA.

Kolesárová, A., Mesiar, R., Mordelová, J., and Sempi, C. (2006). Discrete copulas. *IEEE Trans. Fuzzy Syst.* 14: 698—705.

Kuzmenko, V., Salam, R., and Uryasev, S. (2020). Checkerboard copula defined by sums of random variables. *Depend. Model.* 8: 70—92.

Li, X., Mikusiński, P., Sherwood, H., and Taylor, M. (1997). On approximation of copulas. In: *Distributions with given marginals and moment problems*. Springer, Dordrecht, The Netherlands, pp. 107—116.

Marti, G., Nielsen, F., and Donnat, P. (2016). Optimal copula transport for clustering multivariate time series. In: *2016 IEEE international conference on acoustics, speech and signal processing (ICASSP)*. IEEE, pp. 2379—2383.

Nelsen, R. B. (2006). *An introduction to copulas*. Springer, New York, NY, USA.

Papadakis, N., Peyré, G., and Oudet, E. (2014). Optimal transport with proximal splitting. *SIAM J. Imag. Sci.* 7: 212—238.

Patton, A. J. (2012). A review of copula models for economic time series. *J. Multivariate Anal.* 110: 4—18.

Perrone, E., Solus, L., and Uhler, C. (2019). Geometry of discrete copulas. *J. Multivariate Anal.* 172: 162—179.

Peyré, G. and Cuturi, M. (2019). Computational optimal transport: with applications to data science. *Found. Trends Mach. Learn.* 11: 355—607.

Santambrogio, F. (2015). *Optimal transport for applied mathematicians*. Birkhäuser/Springer International Publishing, Cham, Switzerland.

Scarsini, M. (1984). On measures of concordance. *Stochastica* 8: 201—218.

Schmid, F., Schmidt, R., Blumentritt, T., Gaißer, S., and Ruppert, M. (2010). Copula-based measures of multivariate association. In: *Copula theory and its applications: proceedings of the workshop held in Warsaw, 25—26 September 2009*. Springer, pp. 209—236.

Schoelzel, C. and Friederichs, P. (2008). Multivariate non-normally distributed random variables in climate research—introduction to the copula approach. *Nonlinear Process. Geophys.* 15: 761—772.

Sklar, M. (1959). Fonctions de répartition à n dimensions et leurs marges. *Publ. Inst. Stat. Univ. Paris.* 8: 229—231.

Tootoonchi, F., Haerter, J. O., Räty, O., Grabs, T., Sadegh, M., and Teutschbein, C. (2020). Copulas for hydroclimatic applications—a practical note on common misconceptions and pitfalls. *Hydrol. Earth Syst. Sci. Discuss.* 2020: 1—31.

Villani, C. (2008). *Optimal transport: old and new*, 338. Springer, Berlin and Heidelberg, Germany.

Yuan, Z., Wang, J., Worrall, D., Zhang, B.-B., and Mao, J. (2018). Determining the core radio luminosity function of radio agns via copula. *Astrophys. J. Suppl. Ser.* 239: 33.